International Journal of Science and Research Archive
eISSN: 2582-8185
Cross Ref DOI: 10.30574/ijsra
Journal homepage: https://ijsra.net/

(Research Article)

Check for updates

Advanced geospatial analytics for evapotranspiration dynamics: Integration of Sentinel-1A and FAO Penman-Monteith method

Selvaprakash Ramalingam *

Visiting Research Scholar, Agricultural and Biological Engineering, Purdue University, USA.

International Journal of Science and Research Archive, 2024, 13(02), 3481-3492

Publication history: Received on 13 November 2024; revised on 22 December 2024; accepted on 24 December 2024

Article DOI: https://doi.org/10.30574/ijsra.2024.13.2.2581

Abstract

Evapotranspiration (ET0) is vital for agriculture and environmental management, facing challenges from climate change. Optical remote sensing overcomes reliance on weather station data. The modeled ET0 using the FAO Penman-Monteith method and Partial Least Squares Regression on Sentinel-1A data with 2016-2017 meteorological archives. Comparative analyses revealed stability in transportation areas within deciduous forests and wetlands, contrasting temporal variations. ET0 was significantly influenced by relative humidity (RH) (70.80% to 89.89%), with temperature (T) playing a crucial role. Urban vegetated areas maintained stable T values (29.37°C), while forests exhibited dynamic T variations (24.24°C to 28.94°C). VH polarization captured diverse climatic influences, resulting in a broader range of dynamic ET0 values (7.38 to 10.76 mm/day) compared to VV polarization (6.74 to 9.34 mm/day). VH sensor performance varied; in October 2016 showed moderate accuracy R2 was 0.50 with slight underestimation Bias -0.08, while exceptional accuracy was seen in December 2017 R2 was 1.00 with positive bias (0.57) and excellent agreement KGE was 0.92. VV sensors in October 2016 had a firm fit R2 was 0.55, with moderate underestimation Bias -0.87, and in December 2017 displayed a good fit the R2 was 0.57, with slight overestimation Bias 0.44, and good agreement KGE 0.44. Integrating machine learning and satellite imagery enhances ET0 accuracy for real-time monitoring in adaptive management, addressing climate change, and showcasing sensor-specific variations. Future research should integrate multi-source synthetic aperture radar satellite data and machine learning for precise ET0 estimation in adaptive environmental management.

Keywords: Evapotranspiration; Temperature; Relative Humidity; Sentinel 1A

1. Introduction

Evapotranspiration (ET_0) is crucial for agricultural and environmental management as it quantifies the amount of water lost from the soil and vegetation through evaporation and transpiration. However, it presents challenges in the face of climate change, spatial variability, and the need for Land Use-specific ET_0 estimates in agriculture, forestry, and water management. Weather station data can be scarce and inadequate for ET_0 calculations. The FAO-56 PM model, specifically the Penman-Monteith Method, is a standardized approach for calculating ET_0, which relies on comprehensive weather data. However, the cost of setting up and maintaining weather stations, even in developed countries, presents a significant challenge [1, 2]. The Penman–Monteith Method uses air T, RH, solar radiation (SR), wind speed (WS), atmospheric pressure (ea), and soil heat flux (G) to estimate evapotranspiration. Automated weather stations are scarce, making it challenging to collect accurate weather data due to uncertainties in the information collected [3, 4]. Old and unused weather stations may produce inaccurate data, requiring calibration for quality control [5]. Remote sensing (RS), especially from polar-orbiting satellites, provides relatively frequent and spatially contiguous measurements for global monitoring of surface biophysical variables affecting ET_0, including albedo, vegetation type and density. RS-based mapping of ET_0 is a cost-effective way to estimate and monitor this flux. Since optical RS is hindered in the cloudy region, microwave RS can be inevitable to meet the present demand in ET_0 estimation [6].

* Corresponding author: Selvaprakash Ramalingam

Sentinel-1A and B are Synthetic Aperture Radars (SARs) operated by the European Space Agency, they have been providing detailed images of land use and land cover since 2014 and can aid in assessing ET_0 [7]. [8] investigated the potential of different polarizations (VH, VV) and the VV/VH ratio, along with incidence angles, in predicting significant ET_0 dates [9, 10]. In addition, [11] reported that the ascending pass of SAR backscatter of coniferous forest is more sensitive to the biophysical property evapotranspiration under some scenarios. [12, 13] used a regression modeling technique to predict ET_0 in Malaysia. They used T, humidity, and SR as input variables and found that the model was effective in managing water resources. Their study highlighted the importance of using ET_0 as a predictor variable in regression models for estimating crop water requirements. By analyzing the correlation between ET_0 and optical vegetation indices, researchers have indirectly established a link between Sentinel-1 backscatters and ET_0. Studies by [14, 15] found significant correlations between ET_0 and radar backscatter. However, the study conducted by [14] had limitations in terms of the number of acquisitions, and it remains to be explored whether there is a direct correlation between Sentinel-1 backscatters and ground-based and remotely sensed ET_0 for forested areas over a more extended period. In this context, the main objectives of the study were

- To investigate the spatiotemporal dynamics of Evapotranspiration (ET_0) across diverse land cover types, focusing on understanding the impact of relative humidity (RH), temperature (T), and Sentinel-1A polarization channels (VV and VH sigma naught values).
- To develop a robust land-use-specific Evapotranspiration (ET_0) estimation model by integrating meteorological parameters and Sentinel-1A SAR data.
- To evaluate machine learning and high-res satellite imagery for real-time ET_0 monitoring in agriculture, addressing climate change and spatial variability

2. Material and methods

2.1. Study area and data source

The research focused on the districts along the East Coast of Tamil Nadu in India, as shown in Figure 1. This region is well-known for its vast water bodies, which consist of numerous ponds and lakes. The soil in this particular region is a blend of red and black soil types, which creates unique opportunities for agriculture. The area experiences abundant RF and has excellent water retention capabilities. The average T in this region of Tamil Nadu is approximately 28.1°C, which makes it suitable for a variety of activities. On average, the region experiences around 912 millimeters of RF annually, and the RH usually stays at about 82 percent (en.climate-data.org). In order to calculate ET0 for a region, data from the archives of the Public Works Department (PWD) for the period of 2016-2017 was collected. This data included monthly information on SR, RF, T, RH, and WS. The GEE interface with Java Script was utilized to download monthly mean VV and VH polarization data from Sentinel 1A, with a spatial resolution of 20 meters.

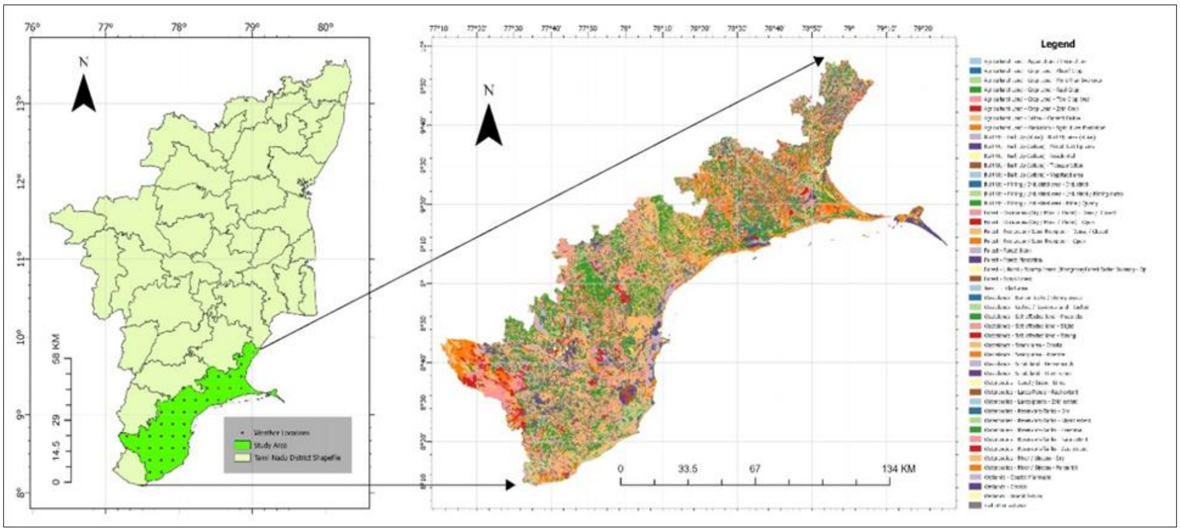

Figure 1 Geographic Snapshot: Depicting the region of interest with marked locations for weather data collection. Weather Stations: Highlighting specific points representing locations where weather data is recorded - land Use Visualization: Illustrating the land use and land cover characteristics within the study area

2.2. Statistical Analysis

We conducted research analysis using several Python libraries to perform comprehensive analyses on both satellite and weather data. The primary libraries utilized rasterio, geopandas, pandas, NumPy, matplotlib.pyplot, scipy.spatial.cKDTree, and Fiona. Together, these libraries provided a robust set of tools for handling geospatial data, conducting spatial analyses, and visualizing results. Rasterio was essential in efficiently reading and processing raster data, particularly satellite imagery. It came with advanced features such as masking, which allowed for precise information extraction based on spatial constraints. The integration of geopandas has been instrumental in managing and manipulating geospatial datasets, achieving seamless compatibility between vector and raster data—the scipy.spatial.cKDTree module was handy for conducting spatial queries and identifying nearest-neighbor relationships, especially for analyzing spatial patterns and data dependencies. The combination of shapely.geometry module and Fiona made it possible to create and manipulate geometric objects, which provided a solid foundation for spatial operations and analyses. These tools played a crucial role in defining study areas, extracting relevant features, and conducting geospatial computations. The use of NumPy has been instrumental in carrying out array-based operations and numerical computations. This has significantly improved the efficiency of various data manipulations and analyses. When used in conjunction with matplotlib.pyplot, it has made it easier to create clear and insightful visualizations. As a result, it has become simpler to interpret complex patterns and trends within datasets (source: pypi.org).

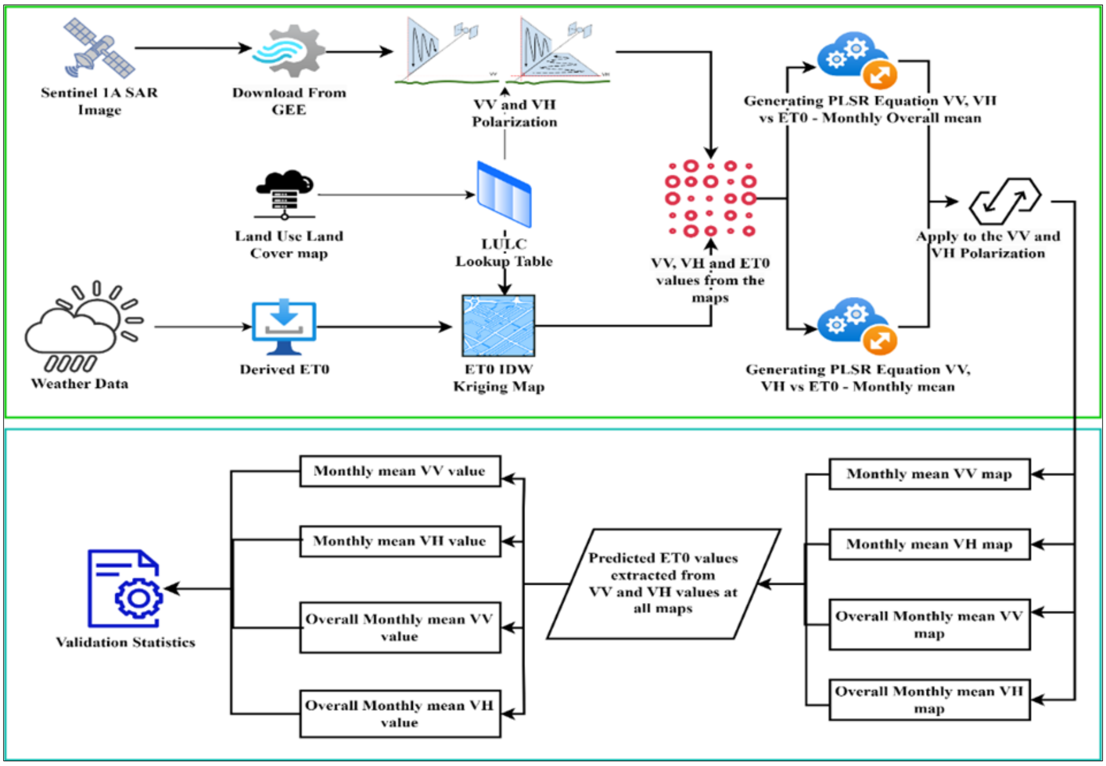

Figure 2 Methodology flow chart

To calculate reference ET0 using the FAO Penman-Monteith method, one must consider several meteorological parameters, including minimum and maximum T, RH, SR, WS, and RF. ETO represents the potential ETO under standard reference conditions, as explained by [16]. Below, each step involved in the calculation process, along with the corresponding equations, is explained (Figure 2).

- Step 1: Calculate Mean T (Tmean)

Tmean = (Tmin + Tmax) / 2

Where Tmean represents the average daily air T.

- Step 2: Calculate Saturation Vapor Pressure (es) and Actual Vapor Pressure (ea) es (Saturation Vapor Pressure) can be calculated using the Clausius-Clapeyron equation or, more accurately, using the Arden Buck equation. es is the maximum amount of water vapor that air can hold at a given T. ea is the actual amount of water vapor in the air. ea (Actual Vapor Pressure) can be calculated using the following equation:

$$ea = (RH/100) \times es$$

Where RH is expressed in percentage

- Step 3: Calculate the Slope of the Vapor Pressure Curve (Δ)

$$\Delta = (4098 \times es) / (Tmean + 237.3)^2$$

Where Δ represents the rate of change of vapor pressure with T.

- Step 4: Calculate the Psychrometric Constant (γ)

$$\gamma = (0.00163 \times P) / \lambda$$

Where γ is the psychrometric constant, which relates the vapor pressure deficit to the actual T; P is atmospheric pressure (kPa); and λ is the latent heat of vaporization (MJ/kg).

- Step 5: Calculate ETO

$$ETO = (0.408 \times \Delta \times (Sr - 0) + \gamma \times 900 / Tmean + 273) \times U2 \times (es - ea)) / (\Delta + \gamma \times (1 + 0.34 \times U2))$$

Where ETO: Reference ETO (in millimeters per day); 0.408: A constant used in the equation; Δ: The slope of the vapor pressure curve (in kPa/°C); γ: The psychrometric constant (in kPa/°C); 900: A constant; Tmean: Mean daily air T at 2 meters height (in °C); es: Saturated vapor pressure (in kilopascals); ea: Actual vapor pressure (in kilopascals); U2: WS at 2 meters height (in meters per second).

Partial Least Squares Regression (PLSR) is a statistical method that models the relationship between predictor variables and a response variable. In the case of predicting ET0 (reference ETO) based on Sentinel-1A VV and VH sigma naught values, the method uses ETO values extracted from an Inverse Distance Weighting (IDW) map of a Land Use Land Cover (LULC) lookup table (Ergon, 2014).

PLSR equation:

VV: Sentinel-1A VV sigma naught values

VH: Sentinel-1A VH sigma naught values

Equations were developed to predict ET0 using various approaches, including monthly mean datasets and overall study period mean. These approaches provided a more complete understanding of the correlations between variables and gave valuable insights into how different factors affect ET0 over time. The first approach involved calculating monthly mean values using equations to consider the temporal variability of ET0.

$$ET0 = b0 + b1 * VV * IDW\_ ET0 \text{ (for VV\_Band)}$$

$$ET0 = b0 + b2 * VH * IDW\_ ET0 \text{ (for VH\_Band)}$$

The monthly impact of VV and VH on ETO showed seasonal patterns and interdependencies. The second method, which utilized mean values over the entire study period, provided a more comprehensive understanding of the correlation between the variables.

$$ETO = b0 + b1 * VV * IDW\_ ET0 \text{ (for VV\_Band)}$$

Where b0: The intercept or constant term; b1: The coefficient for the VV variable; b2: The coefficient for the VH variable; The coefficient for the IDW_ ET0 variable

A method that integrated both short-term oscillations and long-term trends was used to determine the average effect of variables on ET0 during the study period. This approach provided a complete understanding of how VV and VH impact ET0. To conduct this analysis, it was essential to use software or programming languages with PLSR capabilities. Python was one such language, which had libraries like scikit-learn that could be utilized. To perform the analysis, a comprehensive dataset containing historical data of ET0, VV, VH, LULC, and IDW_ ETO was required. Once the dataset was available, the PLSR model automatically estimated the coefficients associated with each variable.

The coefficient of determination (R-squared or R^2) is a measure of how well a linear regression model explains the variance in the dependent variable (Ozer, 1985). It was calculated as follows:

$$R^2 = 1 - (SSR / SST)$$

Where R^2 is the coefficient of determination, SSR is the sum of the squared residuals, and SST is the total sum of squares.

The coefficients in a PLSR model are essential as they indicate the strength and direction of the relationships between ET0 and the predictor variables. Once the model is trained successfully, these coefficients can be used to predict ET0 for new data points. To obtain accurate estimates of ET0, one must input the VV, VH, LULC, and IDW_ ETO values for the new data points into the established PLSR equation.

The Root Mean Square Error (RMSE) is a crucial metric for evaluating the accuracy of ET0 estimates from satellites. In the context of evapotranspiration, precise estimations are essential for understanding water consumption in agricultural and environmental settings. RMSE provides an average measure of the magnitude of errors between observed and predicted ET0 values. It is essential to minimize RMSE to enhance the reliability of satellite-based ET0 models. This ensures that the estimated values closely align with actual observations, making the models more trustworthy [17].

$$RMSE= \sqrt{(1/n) \sum_{(i-1)}^{n} (y_i - \hat{y}_i)^2}$$

Bias: When analyzing estimates of ET0 from satellite data, it is crucial to consider the bias in the model. Bias is an indicator of whether the model consistently overestimates or underestimates the ET0 values. A well-calibrated ET0 model should aim to minimize the bias to ensure that the average predicted value closely matches the average observed value [18].

$$Bias= 1/n \sum_{(i-1)}^{n} (y_i - \hat{y}_i)$$

KGE is a metric that is used to evaluate the correlation, bias, and variability of Satellite ET0 estimates. Accurate estimations of evapotranspiration are crucial for efficient water resource management. KGE provides a comprehensive assessment of model performance, taking into account not only the correlation between observed and estimated values (r), but also the relative variability and bias in the data. A high KGE value indicates a well-performing model, which is essential for reliable satellite-based ETO predictions [19].

$$KGE= \sqrt{(r-1)^2+(s-1)^2+(b-1)^2}$$

3. Results

3.1. Temporal Dynamics of Different Weather Parameters Across Diverse Land Cover Types during the Years 2016 and 2017

The analysis of Sentinel-1A data for evapotranspiration across different land cover types in 2016 and 2017 has revealed some significant temporal dynamics. Built-up (urban) transportation areas have maintained stability with consistently low RF at around 1.09. On the other hand, built-up (urban) vegetated areas exhibited fluctuations, with the highest peak occurring in February 2016 (2.58) and February 2017 (1.40). Forest categories, notably deciduous-dense/closed and evergreen/semi-evergreen-dense/closed, showed varying RF values, indicating seasonal changes. Different types of land cover showed varying fluctuations in their characteristics during different months. For instance, in June 2017, Salt-affected land had a notable RF value of 12.31, whereas Wastelands like Barren Rocky/Stony waste and Gullied/Ravenous land displayed fluctuations. RH patterns also varied across different types of land cover and months. In January 2016, deciduous forests had an RH value of 80.62, while Evergreen forests showed fluctuations in RH values from 74.06 to 77.07. Wastelands, Barren Rocky, and Gullied lands exhibited RH values ranging from 77.18 to 88.55. The

RH values in Coastal and Riverine sandy areas ranged from 82.95 to 89.89. Inland Natural wetlands exhibited RH fluctuations ranging from 78.48 to 84.73. Solar Radiation analysis revealed distinct patterns across land cover categories. Temperature variations were also observed. Wind speed observations indicated stability in urban transportation areas. Urban areas with vegetation showed seasonal fluctuations. Mining and industrial regions, dense deciduous forests, and littoral/swamp forests displayed varying wind speed patterns. Water bodies experienced seasonal fluctuations, and wetlands demonstrated different wind speed characteristics.

3.2. ET0 Analysis Across Land Cover Categories and Months

Interesting patterns emerged when analyzing ET_0 values across different land cover categories and months. In January 2016, Built-Up - Mining/Industrial Area - Industrial/Mining Dump had the lowest ET_0 value of approximately 8.09, while Forest - Deciduous recorded the highest value in February 2016 at about 7.93. Notably, there were no available ET_0 values for Forest - Evergreen/Semi-Evergreen - Dense/Closed. However, Forest - Littoral/Swamp Forest recorded the highest ET_0 value at approximately 10.84 in November 2016. Wastelands had varying values with Wastelands - Barren Rocky/Stony Waste peaking at 10.20 in September 2016. Waterbodies also showed fluctuations, with Waterbodies - Lakes/Ponds - Rabi Extent having the highest ET_0 value at around 9.21 in November 2016.

LULC maps were generated using Sentinel-1A satellite data and ET_0 values. This integration provided a comprehensive understanding of environmental dynamics, enabling precise analysis of water consumption patterns and land surface variations. **Figure** 3a illustrates the consistent trend of lower RF from January to June in 2016 and 2017, with a significant increase from July to December due to the North East Monsoon. **Figure** 3b displays RH variations in the coastal region and terrain from August to February. **Figure** 3c shows the highest SR in the study area from April to August. In **Figure** 3d, the coastal area consistently had high Ts exceeding 24.5 degrees Celsius, while the hill region recorded lower Ts from October to January. **Figure** 3e depicts varying wind patterns across seasons, and **Figure** 3f shows ET_0 values in 2016 and 2017, reflecting seasonal variations influenced by RF patterns and seasonal transitions.

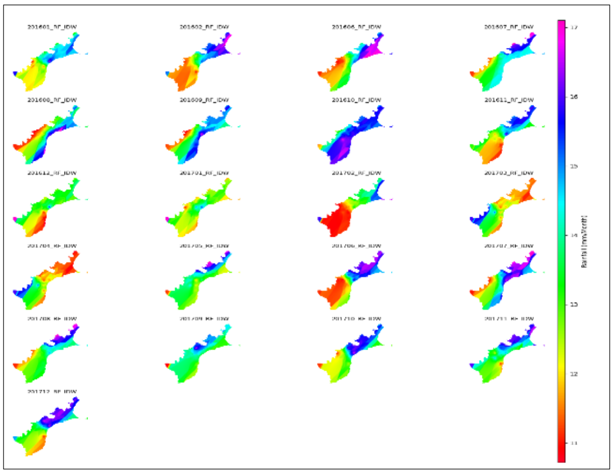

Figure 3a: The map distinctly illustrates the annual RF pattern from January to June in both years, indicating a similar trend with lower RF during these months.

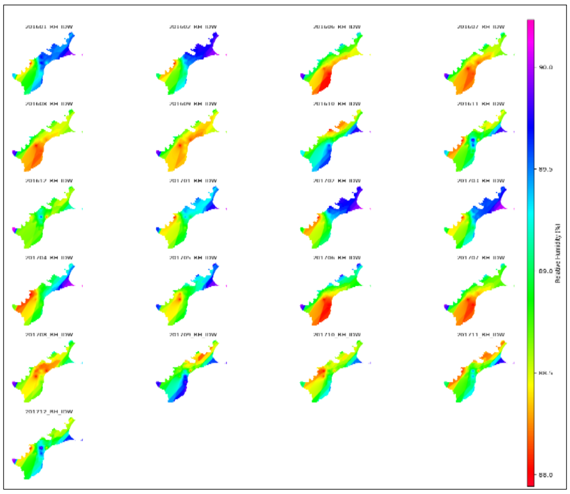

Figure 3b: From August to February, the coastal region experiences higher RH compared to the terrain region.

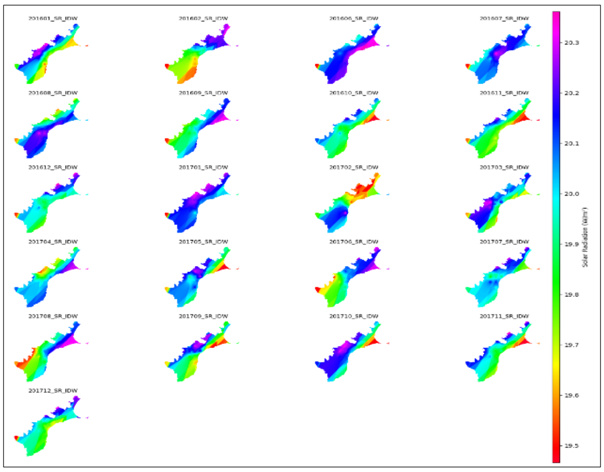

Figure 3c During April to August, the study area receives the highest SR, and a consistent pattern is observed based on the LULC in both 2016 and 2017.

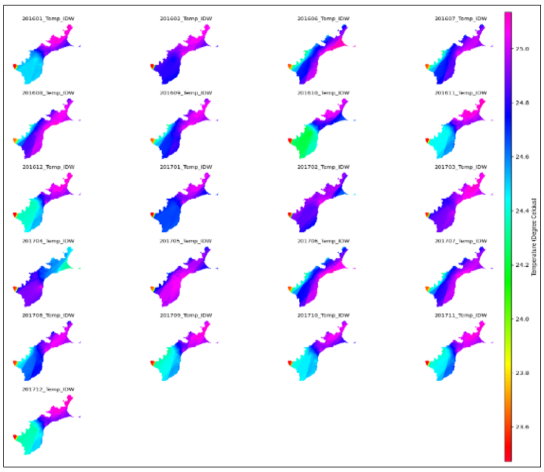

Figure 3d The coastal area of the study consistently experiences high Ts, exceeding 24.5 degrees Celsius on all observation dates.

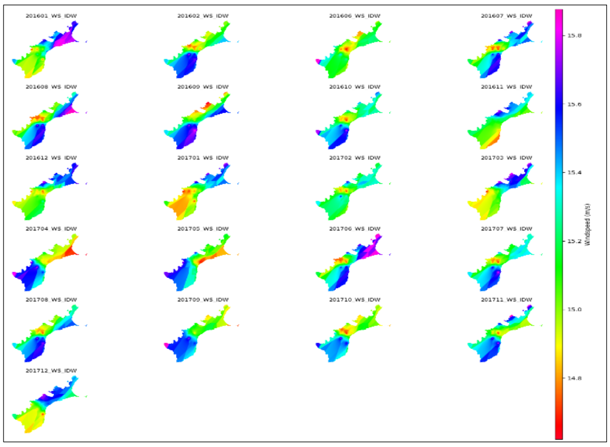

Figure 3e The wind pattern varies across seasons. During January, February, and March, the WS is notably lower.

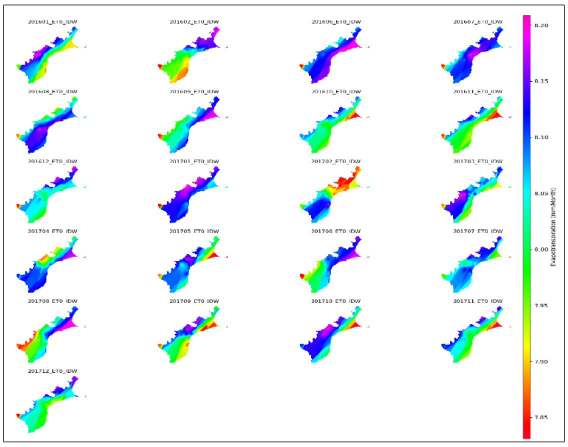

Figure 3f In 2016, the ET_0 values for January, October, November, and December showed a consistent pattern. Similarly, in 2017, the ET_0 values for October, November, and December exhibited a similar trend.

3.3. Using a Monthly Mean Equation-Based ETO Map on Sentinel-1A VH Polarization

The analysis of ET_0 values using Sentinel-1A VH polarization data has revealed distinct patterns that offer valuable insights into environmental dynamics. Notably, March and May 2017 stood out with significantly high ET_0 values, indicating intensified processes during these periods. Meanwhile, moderate ET_0 values were observed in June, July, and August 2016, as well as in January, February, September, November, and December 2017. These suggest a more balanced water loss. On the other hand, low ET_0 values were recorded in June, September, October, November, and December 2016, and April, June, July, August, and October 2017. These align with reduced water loss, which could be influenced by factors such as reduced solar radiation. In agricultural lands, ET_0 values varied, implying varying water requirements. Evergreen forests showed diverse climatic influences, while littoral and swamp forests indicated a distinct climatic environment. Gullied wastelands displayed substantial variability in water loss, and water bodies exhibited fluctuations highlighting seasonal and environmental impacts. The ET_0 values derived from Sentinel-1A VH polarization data provided nuanced insights into the intricate interplay between vegetation, water dynamics, and atmospheric conditions across different land categories.

3.4. Using a Monthly Mean Equation-Based ETO Map on Sentinel-1A VV Polarization

The analysis of ET_0 values, derived from the Sentinel-1A VV band and using PLSR monthly mean equations, has revealed distinct patterns for various months and years. The high ET_0 months in 2016 (February, June, July, August, December) and 2017 (January, April, December) have indicated an increase in water loss. Moderate values were identified in 2017 (February, March, October, and November), while low ET_0 occurred in April and September of 2017. During specific months of 2016 and 2017, shallow ET_0 values were observed, suggesting minimal water loss during those periods (**Figure 5**). The coupled use of the Sentinel-1A VV band and PLSR monthly mean equations has provided a comprehensive understanding of ET_0 variability, which is crucial for assessing water management strategies and understanding the impact of environmental factors on ET_0 dynamics across different land classes.

3.5. Utilizing an Overall Mean Equation-Based ETO Map on Sentinel-1A VH Polarization

The analysis of ET_0 using Sentinel-1A VH band data revealed distinct patterns across different months in 2016 and 2017. Moderate ET_0 values persisted during specific months in both years, with a shift observed in low ET_0 months between 2016 and 2017. The use of PLSR allowed for the exploration of relationships between Sentinel-1A VH band data and ET_0, providing comprehensive insights into factors influencing ET_0 dynamics. In December 2016, Sentinel-1A VH polarization output revealed varying minimum and maximum ET_0 values across diverse land classes. Agricultural lands dedicated to Aquaculture/Pisciculture exhibited dynamic environmental conditions, while Evergreen/semi-evergreen open areas displayed nuanced moisture and temperature dynamics. Littoral/Swamp Forests provided insight into unique ecological conditions, and Gullied/Ravine Wastelands showcased environmental heterogeneity. Waterbodies displayed varying ET_0 values (ranging from 6.81 to 9.30), with potential variations emphasized in specific instances. Coastal manmade wetlands showed relatively consistent ET_0 (8.14), indicating stability. Sentinel-1A outputs provided valuable insights into the dynamic nature of ET_0 across different land classes, highlighting unique environmental conditions influencing these variations.

3.6. Utilizing an Overall Mean Equation-Based ETO Map on Sentinel-1A VV Polarization

In the study area, the analysis of ET_0 identified two distinct categories: High ET_0 months and Moderate ET_0 months. The Moderate ET_0 months were extracted from Sentinel-1A VV band data using PLSR. The Overall Mean Equation resulting from Moderate ET_0 months in 2017 (April, September, October, and November) served as a robust model for predicting ET_0 values based on Sentinel-1A VV polarization. In agricultural lands dedicated to aquaculture, ET_0 values showed a narrow range, indicating stability in environmental conditions for aquatic cultivation. Evergreen and semi-evergreen forests with an open canopy displayed a slightly broader spectrum, indicating variations in transpiration and evaporation rates. Gullied or ravine-like wastelands showed notably consistent ET_0 values, suggesting a uniform pattern of aridity, while salt-affected wastelands exhibited a discernible range, possibly influenced by saline content. Water bodies, such as lakes and ponds, revealed diverse ET_0 values, indicating varying moisture exchange influenced by depth, temperature, and surrounding vegetation. Coastal man-made wetlands exhibited a singular data point, implying a stable environment with minimal ET_0 fluctuations (**Figure 7**). The Sentinel-1A data provided nuanced insights into ET_0 dynamics across different land classes, revealing patterns of stability, variability, and environmental influences on moisture exchange

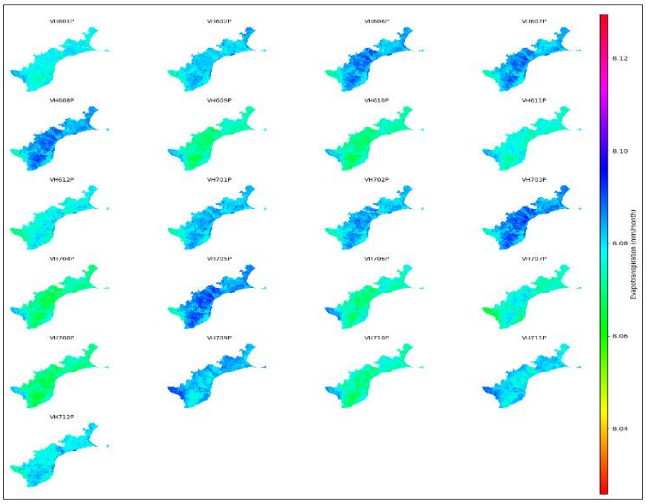

Figure 4 Using a monthly mean equation-based ET_0 map on Sentinel-1A VH polarization

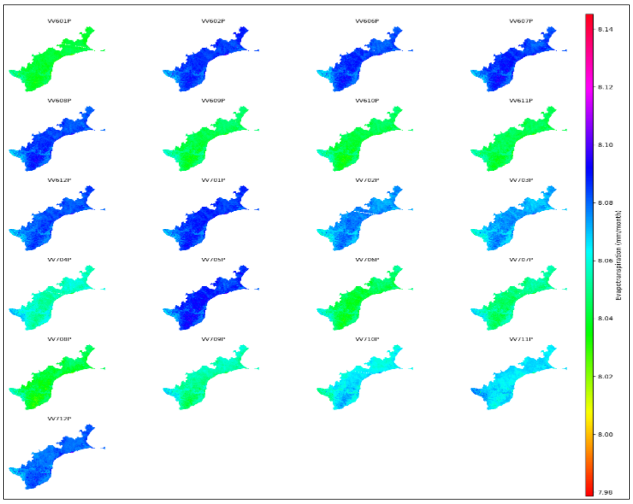

Figure 5 Using a monthly mean equation-based ET_0 map on Sentinel-1A VV polarization

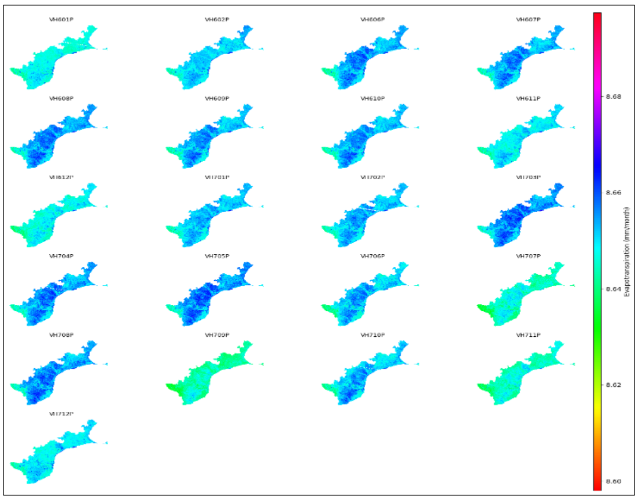

Figure 6 Utilizing an overall mean equation-based ET_0 map on Sentinel-1A VH polarization

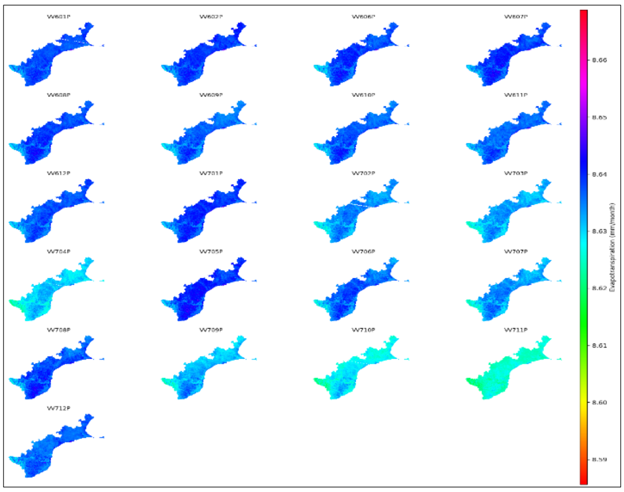

Figure 7 Utilizing an overall mean equation-based ET_0 map on Sentinel-1A VV polarization

3.7. Temporal Dynamics and Model Performance: Sentinel 1A Monthly Mean Equation vs Overall Mean Equation

Table 1 Temporal Dynamics and Model Performance: Sentinel 1A Monthly Mean Equation vs Overall Mean Equation

Months	VH Polarization				VV Polarization			
	R-squared	RMSE	Bias	KGE	R-squared	RMSE	Bias	KGE
Jan-16	0.48	0.20	0.20	-0.72	0.50	0.24	0.24	-1.00
Feb-16	0.37	0.32	0.32	0.23	0.47	0.33	0.33	0.15
Jun-16	0.51	1.01	1.01	0.18	0.54	1.02	1.02	0.11
Jul-16	0.48	0.79	0.79	0.33	0.50	0.78	0.78	0.66
Aug-16	0.47	0.39	0.39	0.13	0.52	0.41	0.41	0.09
Sep-16	0.49	0.55	0.55	-0.85	0.56	0.49	0.49	-0.91
Oct-16	0.50	0.08	0.08	-0.77	0.55	0.06	0.06	-0.87
Nov-16	0.40	0.68	0.68	-0.77	0.47	0.63	0.63	-0.83
Dec-16	0.39	0.56	0.56	0.47	0.47	0.56	0.56	0.38
Jan-17	0.42	0.33	0.33	-3.10	0.50	0.36	0.36	0.70
Feb-17	0.43	0.67	0.67	0.46	0.49	0.66	0.66	0.66
Mar-17	0.47	1.55	1.55	0.43	0.52	1.52	1.52	0.46
Apr-17	0.45	2.11	2.11	-1.37	0.48	2.11	2.11	-0.73
May-17	0.45	0.46	0.46	0.48	0.48	0.47	0.47	0.32
Jun-17	0.46	1.26	1.26	-0.75	0.51	1.22	1.22	-0.81
Jul-17	0.46	0.58	0.58	-2.07	0.51	0.57	0.57	-6.71
Aug-17	0.46	0.72	0.72	-0.87	0.51	0.64	0.64	-0.92
Sep-17	0.52	0.37	0.37	-0.83	0.54	0.32	0.32	-0.88
Oct-17	0.52	0.52	0.52	-1.69	0.57	0.49	0.49	-3.73
Nov-17	0.45	1.86	1.86	-0.81	0.54	1.79	1.79	-0.84
Dec-17	1.00	0.57	0.57	0.92	0.57	0.56	0.56	0.44

Source: Authors calculated using Sentinel 1A Monthly Mean Equation vs Overall Mean Equation output

3.7.1. VH Sensors

The analysis of data from Sentinel-1A for ET_0 estimation showed varying performance across different months, as presented in Table 1. In October 2016, the sensor demonstrated a moderate R^2 value of 0.50, which means that 50% of the variance in ET_0 was explained. Despite a low RMSE of 0.08, a negative bias (-0.08) suggested a slight underestimation. The KGE of -0.77 indicated moderate agreement with the observed ET_0. Moving to November 2016, the R^2 value dropped to 0.40, with a higher RMSE of 0.68 and a negative bias (-0.68), indicating more significant errors and continued underestimation. The results for December 2016 showed an improvement with an R^2 value of 0.39, a moderate RMSE of 0.56, and an optimistic bias of 0.47. These values suggested that the estimate was reasonably accurate and showed good agreement with a KGE value of 0.47. However, in October 2017, the sensor exhibited a relatively high R^2 value of 0.52 but a low KGE value of -1.69, which indicates poor agreement despite a low RMSE value. On the other hand, December 2017 showed exceptional performance with a perfect fit R^2 value of 1.00, low RMSE value of 0.57, and optimistic bias of 0.57, indicating accurate ET_0 estimation and excellent agreement with a KGE value of 0.92. In September 2017, the sensor demonstrated a high R^2 value of 0.52, a low RMSE value of 0.37, and a negative bias of -0.83, which suggests underestimation. The KGE value of -0.83 indicates moderate agreement between the estimate and the actual value.

3.7.2. VV Sensors

In October 2016, a strong fit was indicated by the R^2 value of 0.55, complemented by a low RMSE of 0.06 and a negative bias of -0.87, suggesting underestimation. The KGE of -0.87 suggested a moderate level of agreement. However, in October 2017, despite a high R^2 value of 0.57, the data showed a high degree of underestimation, as evidenced by a substantial negative bias of -3.73 and a poor KGE of -3.73, despite a low RMSE of 0.49. Moving to December 2017, the R^2 value of 0.57 indicated a good fit, with a low RMSE (0.56) and a slightly optimistic bias (0.44), implying a slight degree of overestimation. The KGE of 0.44 supported good agreement. On the other hand, in July 2017, an R^2 value of 0.51 suggested a moderate degree of explained variance alongside a moderate RMSE (0.57) and a significant negative bias of -6.71, indicating substantial underestimation. The KGE of -6.71 confirmed poor agreement during this period (**Table 1**). In summary, these findings emphasized the variability in Sentinel-1A-derived evapotranspiration results across different months, highlighting the need for specific contextual factors to be taken into consideration when interpreting the data.

4. Discussion

Analyzing different land covers reveals that deciduous forests and wetlands exhibit changes over time. Humidity levels (RH) range from 70.80 to 89.89 percent, and T varies in forested regions. Sentinel-1A VH Polarization captures a broader range of dynamic ET_0 values across land classes than VV Polarization, indicating its ability to capture diverse climatic influences. RH and surface roughness analyses provide insights into humidity levels and land surface characteristics. The R^2 values for monthly mean ET_0 predictions vary, highlighting the importance of considering specific dates and polarization channels.

A recent study by [20] proposes a new approach for estimating actual evapotranspiration (ETa) fluxes using data from the Sentinel-1A satellite. The approach is beneficial in regions where access to optical Sentinel-2 images is limited during high cloud cover periods, such as the monsoon season. The study evaluates monthly mean and overall mean equations derived from Sentinel-1A's VH and VV bands for predicting ET_0. Both approaches provide valuable insights into the nuanced variations in water loss from soil and vegetation. The researchers found that analyzing moderate ET_0 months in 2017 reveals the significance of the Sentinel-1A VV band in capturing subtle variations during specific periods. The derived ETa estimates showed strong performance, especially during non-monsoon periods, highlighting their usefulness for effective irrigation management during periods of high cloud cover. Overall, the study shows that a Sentinel-1A-based approach can be a valuable tool for estimating ET_0 fluxes in regions with limited access to optical Sentinel-2 images.

During December 2016, analyses of VH band data revealed intricate patterns across different land classes. Agricultural lands dedicated to aquaculture or pisciculture exhibit subtle fluctuations in ET_0 values, suggesting a consistent level of moisture exchange conducive to stable conditions for aquatic cultivation. In evergreen and semi-evergreen forests with an open canopy, a slightly broader spectrum of ET_0 values indicates variations in transpiration and evaporation rates within forested areas. Gullied or ravine-like wastelands display notably consistent ET_0 values, suggesting a uniform pattern of aridity. Salt-affected wastelands show a discernible range in ET_0 values, indicating specialized environmental conditions influenced by saline content. Water bodies, including lakes and ponds, exhibit diverse ET_0 values, hinting at varying levels of moisture exchange influenced by factors such as water depth or surrounding vegetation. Coastal manmade wetlands display a singular data point, indicating a relatively stable environment for these wetlands with minimal fluctuations in ET_0.

A study conducted by [21] utilized machine learning algorithms and Sentinel-2 MSI sensor data to simplify ETrF estimation in sugarcane. This enhances the METRIC model predictions. The study found that approaches at 10m and 20m resolutions, especially with XgbLinear and XgbTree, were more efficient in ETrF estimation compared to traditional methods. On the other hand, SVM had the lowest accuracy [22]. Although there are differences in data resolution from previous studies, the model performs well in predicting ET_0. The established ET_0 model provides a precise means to predict evapotranspiration in semi-arid regions, facilitating effective management [23]. This is particularly useful in situations where weighing-type field lysimeters are not available.

It is necessary to compare the monthly mean and overall mean equations to predict ET_0 accurately. This comparison should be based on the Overall PLSR equations that consider the results of Sentinel-1A VH and VV. The evaluation should assess the ability of each approach to capture variations in ET_0 values across different land classes and its performance in reflecting environmental dynamics. In addition, statistical analyses like correlation coefficients and model accuracy assessments can provide quantitative measures to support the qualitative observations made in this analysis. Ultimately, the preference for the equation may depend on the goals of the study and the environmental conditions influencing ET_0 in the study area.

Python libraries such as NumPy, matplotlib.pyplot and pandas are crucial for efficient handling, processing, and visualization of data throughout the analysis. This research employs comprehensive data and advanced modeling techniques to comprehend the intricate dynamics of ET_0 in different land cover categories, providing valuable insights for land management and environmental monitoring. The Sentinel-1A single-date equation has been proven effective in capturing diverse land cover dynamics, thereby improving environmental monitoring and land planning insights.

5. Conclusion

The study employed satellite-derived parameters to unravel the intricate dynamics of environmental changes in 2016 and 2017. By analyzing climatic variations, land cover types, and seasonal transitions, we identified distinct patterns in soil and vegetation water loss. Categorizing ET_0 months allowed us to explore temporal variations, emphasizing the diverse performances of VH and VV polarization channels. Evaluating Sentinel-1A's equations revealed the importance of a date-specific and polarization-specific approach for accurate predictions. Notably, the study uncovered the significance of VV band in distinguishing moderate ET_0 months in 2017, offering targeted insights. The findings provide valuable contributions to environmental monitoring, land use planning, and water resource management, empowering decision-makers with informed strategies for sustainable practices. The integration of satellite data, statistical models, and environmental parameters establishes a robust framework for future studies, advancing our understanding of Earth's ecosystems

Compliance with ethical standards

Disclosure of conflict of interest

No conflict of interest to be disclosed.

References

[1] Chu R, Li M, Shen S, et al (2017) Changes in Reference Evapotranspiration and Its Contributing Factors in Jiangsu, a Major Economic and Agricultural Province of Eastern China. Water 9:486. https://doi.org/10.3390/w9070486

[2] Shafizadeh-Moghadam H (2023) Utilizing machine learning models with limited meteorological data as alternatives for the FAO-56 model in estimating potential evapotranspiration. Res Sq. https://doi.org/10.21203/rs.3.rs-3324487/v1

[3] Gocic M, Trajkovic S (2010) Software for estimating reference evapotranspiration using limited weather data. Comput Electron Agric 71:158–162. https://doi.org/10.1016/j.compag.2010.01.003

[4] Tabari H, Talaee PH (2011) Local Calibration of the Hargreaves and Priestley-Taylor Equations for Estimating Reference Evapotranspiration in Arid and Cold Climates of Iran Based on the Penman-Monteith Model. J Hydrol Eng 16:837–845. https://doi.org/10.1061/(ASCE)HE.1943-5584.0000366

[5] Raza A, Fahmeed R, Syed NR, et al (2023) Performance Evaluation of Five Machine Learning Algorithms for Estimating Reference Evapotranspiration in an Arid Climate. Water 15:3822. https://doi.org/10.3390/w15213822

[6] Zhang K, Kimball J, Running S (2016) A review of remote sensing based actual evapotranspiration estimation: A review of remote sensing evapotranspiration. WIREs Water 3:834–853. http://dx.doi.org/10.1002/wat2.1168

[7] Colin A, Peureux C, Husson R, et al (2022) Segmentation of Rainfall Regimes by Machine Learning on a Colocalized Nexrad/Sentinel-1 Dataset. In: IGARSS 2022 - 2022 IEEE International Geoscience and Remote Sensing Symposium. pp 307–309

[8] Bogdanovski OP, Svenningsson C, Månsson S, et al (2023) Yield Prediction for Winter Wheat with Machine Learning Models Using Sentinel-1, Topography, and Weather Data. Agriculture 13:813. https://doi.org/10.3390/agriculture13040813

[9] Veloso A, Mermoz S, Bouvet A, et al (2017) Understanding the temporal behavior of crops using Sentinel-1 and Sentinel-2-like data for agricultural applications. Remote Sens Environ 199:415–426. https://doi.org/10.1016/j.rse.2017.07.015

[10] Vreugdenhil M, Wagner W, Bauer-Marschallinger B, et al (2018) Sensitivity of Sentinel-1 Backscatter to Vegetation Dynamics: An Austrian Case Study. Remote Sens 10:1396. https://doi.org/10.3390/rs10091396

[11] Mueller MM, Dubois C, Jagdhuber T, et al (2022) Sentinel-1 Backscatter Time Series for Characterization of Evapotranspiration Dynamics over Temperate Coniferous Forests. Remote Sens 14:6384. https://doi.org/10.3390/rs14246384

[12] Abdel-Fattah MK, Kotb Abd-Elmabod S, Zhang Z, Merwad A-RMA (2023) Exploring the Applicability of Regression Models and Artificial Neural Networks for Calculating Reference Evapotranspiration in Arid Regions. Sustainability 15:15494. https://doi.org/10.3390/su152115494

[13] Elbeltagi A, Srivastava A, Al-Saeedi AH, et al (2023) Forecasting Long-Series Daily Reference Evapotranspiration Based on Best Subset Regression and Machine Learning in Egypt. Water 15:1149. https://doi.org/10.3390/w15061149

[14] El-Shirbeny MA, Abutaleb K (2017) Sentinel-1 Radar Data Assessment to Estimate Crop Water Stress. World J Eng Technol 5:47–55. https://doi.org/10.4236/wjet.2017.52B006

[15] Nasrallah A, Baghdadi N, El Hajj M, et al (2019) Sentinel-1 Data for Winter Wheat Phenology Monitoring and Mapping. Remote Sens 11:2228. https://doi.org/10.3390/rs11192228

[16] Allen RG (1998) Crop Evapotranspiration-Guidelines for Computing Crop Water Requirements-FAO Irrigation and Drainage Paper 56

[17] Montgomery DC, Peck EA, Vining GG (2021) Introduction to Linear Regression Analysis. John Wiley and Sons

[18] Wilks DS (2011) Statistical Methods in the Atmospheric Sciences. Academic Press

[19] Gupta HV, Kling H, Yilmaz KK, Martinez GF (2009) Decomposition of the mean squared error and NSE performance criteria: Implications for improving hydrological modelling. J Hydrol 377:80–91. https://doi.org/10.1016/j.jhydrol.2009.08.003

[20] Chintala S, Harmya TS, Kambhammettu BVNP, et al (2022) Modelling high-resolution Evapotranspiration in fragmented croplands from the constellation of Sentinels. Remote Sens Appl Soc Environ 26:100704. https://doi.org/10.1016/j.rsase.2022.100704

[21] dos Santos RA, Mantovani EC, Fernandes-Filho EI, et al (2022) Modeling Actual Evapotranspiration with MSI-Sentinel Images and Machine Learning Algorithms. Atmosphere 13:1518. https://doi.org/10.3390/atmos13091518

[22] Sammen (2023) Predicting reference evapotranspiration in semi-arid-region by regression- based machine learning methods using limited climatic inputs. https://www.researchsquare.com. Accessed 28 Dec 2023

[23] Rajput J, Singh M, Lal K, et al (2023) Data-driven reference evapotranspiration (ET0) estimation: a comparative study of regression and machine learning techniques. Environ Dev Sustain. https://doi.org/10.1007/s10668-023-03978-4.